



## Supported oxorhenate catalysts prepared by thermal spreading of metal Re<sup>0</sup> for methanol conversion to methylal

Xavier Sécordel<sup>a</sup>, Anthony Yoboué<sup>a</sup>, Sylvain Cristol<sup>a</sup>, Christine Lancelot<sup>a</sup>, Mickaël Capron<sup>a</sup>, Jean-François Paul<sup>a</sup>, Elise Berrier<sup>a,b,\*</sup>

<sup>a</sup> Unité de Catalyse et de Chimie du Solide UMR CNRS 8181 Université Lille 1 Sciences et Technologie, F-59655 Villeneuve d'Ascq Cedex, France

<sup>b</sup> CNRS, Centre National de la Recherche Scientifique, France

### ARTICLE INFO

#### Article history:

Received 20 July 2011

Accepted 1 August 2011

Available online 19 August 2011

#### Keywords:

Raman

Rhenium

TiO<sub>2</sub>

SiO<sub>2</sub>

Methanol

### ABSTRACT

TiO<sub>2</sub>-anatase and SiO<sub>2</sub> supported oxorhenate catalysts were prepared by an original and simple technique based on the oxidative dispersion of metallic rhenium under dry conditions. The dispersion process of the supported oxorhenate phase as a function of the rhenium coverage and the support properties are discussed on the base of *in situ* characterization. The structures of the as prepared catalysts were found to be comparable to those of materials prepared using the incipient wetness impregnation technique. The absence of water in the preparation technique has made it possible to highlight the role of the hydration level on the rhenium oxide volatilization. The as-prepared Re/TiO<sub>2</sub> catalysts were found to be effective for the direct conversion of methanol to methylal.

© 2011 Elsevier Inc. All rights reserved.

### 1. Introduction

As affordable from biomass degradation [1], the methanol is becoming a smart source for formaldehyde [2], dimethyl ether, methylformate [3] and dimethoxymethane (methylal) [3,4] production. The latter is attracting growing attention as model reaction for direct ethanol conversion to diethoxyethane (acetal). The direct conversion of methanol to dimethoxymethane (DMM or methylal) involves the oxydation of methanol to formaldehyde and subsequent condensation of two methanol molecules with formaldehyde.

The simpler efficient system is anatase-TiO<sub>2</sub> supported oxorhenate as evidenced by Iwasawa and coworkers [5,6] and further development of several rhenium-containing efficient catalysts for the direct selective oxidation of methanol to methylal was recently reported [7].

The classical technique for preparing a supported oxorhenate is the wetness impregnation of a given support followed by ageing, drying and calcination steps. The structure under ambient and dehydrated conditions of such catalysts was thoughtfully investigated [8–10] and was found to retain several structures where the rhenium stands in tetrahedral coordination. Another preparation method was reported based on the chemical vapor deposition (CVD) of methyltrioxorhenium, CH<sub>3</sub>ReO<sub>3</sub>. In this

procedure, the support was heated under vacuum and subsequently exposed to the vaporized CH<sub>3</sub>ReO<sub>3</sub> [11,12]. An approaching process using gaseous Re<sub>2</sub>O<sub>7</sub> was reported by Lacheen and coworkers [13] to afford Re-oxo species grafted onto H-MFI zeolite. The structure of such catalysts was found to be essentially monomeric and based on a mixed Si–Al grafting with Si–O–ReO<sub>3</sub>–Al bonds. These materials were shown to be highly active in selective oxidation of alcohols and alkanes [14]. Supported oxorhenate onto zeolite and  $\gamma$ -alumina were also prepared by physical mixing of the support and ammonium perrhenate, NH<sub>4</sub>ReO<sub>4</sub>, followed by heat treatment at temperatures above 673 K to remove ammonium counter ions [15,16]. The resulting rhenium oxide phase was shown to be well dispersed onto the support surface and the process involved was similar to a thermal spreading. The technique was extended to the preparation of a series of supported oxide catalysts from direct mixing of bulk oxides as V<sub>2</sub>O<sub>5</sub>, Re<sub>2</sub>O<sub>7</sub> or MoO<sub>3</sub> with the support material (Al<sub>2</sub>O<sub>3</sub>, SiO<sub>2</sub>, SnO<sub>2</sub> or TiO<sub>2</sub>) by Wang and coworkers [17]. The authors have proposed that Re<sub>2</sub>O<sub>7</sub> has spread onto the TiO<sub>2</sub> surface during methanol oxidation. Okal and coworkers have prepared  $\gamma$ -alumina supported rhenium catalysts by the conventional wetness impregnation technique. After due calcination, they have examined the properties of such materials along sintering by reduction up to 800 °C in H<sub>2</sub> and subsequent reoxidation in O<sub>2</sub> [18–20].

Regardless of the preparation technique, the structure of TiO<sub>2</sub>-anatase supported rhenium oxide catalyst is reported to be essentially made of monomeric, tetrahedrally coordinated species featured by a sharp and intense terminal Re=O<sub>t</sub> stretching mode,

\* Correspondence to: Université des Sciences et Technologies de Lille, Unité de Catalyse et de Chimie du Solide, Bât C3, Cité Scientifique, 59655 Villeneuve d'Ascq Cedex, France. Fax: +33 3 20 43 65 61.

E-mail address: [Elise.Berrier@univ-lille1.fr](mailto:Elise.Berrier@univ-lille1.fr) (E. Berrier).

$\nu_{\text{S(Re=O)}}$  observed around 1000–1010  $\text{cm}^{-1}$  under dehydrated conditions [21–24]. Concerning  $\text{Al}_2\text{O}_3$ -supported rhenium materials, two distinct molecular structures were identified under dehydrated conditions according to the surface coverage [19,21]. Because of the high volatility of rhenium oxide and the soft rhenium to  $\text{TiO}_2$  bonding, the monolayer level is not expected for  $\text{Re}/\text{TiO}_2$  catalysts and it is admitted that the supported phase mainly consists of isolated species [10]. However, recent studies have suggested that under selected conditions, oligomeric rhenium oxide can be present at the surface of anatase [9].

Based on these considerations and having in mind the high volatility of  $\text{Re}_2\text{O}_7$ , we describe here a new synthesis technique based on the oxidative dispersion of metal rhenium onto  $\text{TiO}_2$ -anatase and  $\text{SiO}_2$  (Aerosil200) support. The basis of the technique is a simple mechanical mixing and grinding of mesh Re powder with the support followed by a mild heat treatment under pure oxygen up to 400 °C. Two kinds of processes can occur: direct thermal spreading or a combination of rhenium oxidation and sublimation to  $\text{Re}_2\text{O}_7$  followed by rhenium deposition onto the surface, which could be related to a CVD. In order to discriminate the nature of the support on one hand and its texture on the other hand, we have compared two anatase- $\text{TiO}_2$  supports, which differ according to their textural properties and  $\text{SiO}_2$ -Aerosil200.

## 2. Experimental and methods

### 2.1. Catalyst preparation

The anatase materials, kindly provided by Sachtleben and labeled Hombikat K03 (100  $\text{m}^2 \text{g}^{-1}$ ) and Hombikat F01 (300  $\text{m}^2 \text{g}^{-1}$ ), were vigorously rinsed in distilled water and heated under dry air up to 400 °C to remove any trace of alkaline ions in the structure. This point was checked by elemental analysis (ICP) and XPS. The silica support used in the present study is the Aerosil200 available at Degussa GmbH. The powder was subjected to re-gelation in distilled water, drying and calcination step at 600 °C prior to rhenium enrichment.

The as-prepared supports were mixed with the desired amount of rhenium powder (Puratronic, 99.999%, Alfa Aesar) and manually grinded together in an agate mortar. The resulting light gray mixture was then calcined under pure  $\text{O}_2$  flow (20  $\text{cm}^3 \text{min}^{-1}$ ) up to 400 °C (heating rate: 1 °C  $\text{min}^{-1}$ ). After this step, the catalysts have turned to white.

### 2.2. In situ Raman spectroscopy

The *in situ* spectral analysis was allowed using the environmental spectroscopic chamber developed by Harrick, which we have already described [9]. Micro-Raman spectra were recorded while increasing the temperature under pure oxygen using the 532 nm second harmonic line of a Nd:YAG laser (laser power on the sample: 5 mW). A 50× microscope objective was used to focus the excitation beam (13.6  $\mu\text{m}$  spot) and collect light. The scattered light was collected through a confocal hole (150  $\mu\text{m}$ ) and analyzed by a spectrometer (grating 1800 gr.) and a nitrogen cooled CCD (Labram Infinity, Jobin Yvon).

### 2.3. Thermal analysis

The thermogravimetric analysis (TGA) coupled with differential scanning calorimetry (DSC) was performed using a thermo-analyzer TA Instruments SDT 2960. The temperature was increased from room temperature to 400 °C (rate: 5 °C  $\text{min}^{-1}$ ) under a  $\text{He}/\text{O}_2$  (50:50) flow.

### 2.4. X photoelectron spectroscopy (XPS)

The spectrometer used for the study is the ESCALAB 220 XL from VG Scientific. The  $K\alpha$  line of aluminum (1486.6 eV) was used as X-rays source and the analysis was performed under secondary vacuum ( $10^{-12}$  bar). The decomposition of the experimental photopeaks was done using the software CasaXPS. The atomic relative contents were calculated from the normalized area of the corresponding photopeaks.

### 2.5. Transmission electron microscopy analysis

The TEM analysis of the solids was performed on a Tecnai electron microscope operating at an accelerating voltage of 200 kV.

### 2.6. Diffuse reflectance (DR) UV-visible absorption

DR-UV-visible spectra were collected under ambient conditions using a Perkin-Elmer Lambda 650 spectrometer equipped with an integration sphere. Typically, the samples were diluted 10× in  $\text{BaSO}_4$ . The support, diluted accordingly, was used as 100% reflectance reference, so that the absorbance detected is characteristic of the oxorhenate phase.

### 2.7. Catalytic activity

The catalytic activity was measured in a quartz fixed bed reactor immediately after the *in situ* preparation of catalysts by heating the  $\text{Re}^0/\text{TiO}_2$  mixture up to 400 °C under  $\text{O}_2$ . As a consequence, the materials were not subjected to atmosphere before reaction. After preparation, the catalysts were cooled down to room temperature and the gas feed was allowed through the catalytic bed while increasing temperature. Two reaction temperatures, 200 and 260 °C were chosen. At each temperature, the products were subsequently analyzed after one hour on stream by a  $\mu$ -gas chromatograph (SRA) equipped with a Poraplot U and a 5 A molecular sieve columns and TCD detectors. The typical reaction conditions are the following:  $\text{GHSV} = 26,000 \text{ mL h}^{-1} \text{g}^{-1}$  and  $\text{He}/\text{O}_2/\text{CH}_3\text{OH} = 80/16/4$  (mol%) at 1 atm. In all cases, the carbon balance was comprised between 95% and 105%, which was considered as satisfactory.

## 3. Results

### 3.1. Re leaching during preparation

The rhenium loss during high temperature step of preparation is a well-known phenomenon [25]. Therefore, ICP measurements were performed on the final materials in order to clarify the maximal Re loading affordable by the technique. After the above-mentioned preliminary treatment, the BET surface areas of the studied supports, silica and anatase Hombikat K03 and F01 were found to reach 230, 93 and 254  $\text{m}^2 \text{g}^{-1}$ , respectively. As expected, the rhenium loss is significant, especially at high initial mix concentration, as reported in Fig. 1. Below 8wt% Re loading – or 1.5 atoms  $\text{Re}/\text{nm}^2$  – in the fresh mix, the final values for rhenium content and surface coverage is identical for all samples and follow a linear evolution. Increasing the amount of Re in the preparation over this limit produced a significant Re loss, so that the maximum rhenium coverage for ReA200, ReF and ReK catalysts were found to reach 2.15, 2.4 and 3.1 atoms  $\text{Re}/\text{nm}^2$ , respectively. The latter is 30% greater than the maximal value reported previously [10] for such materials.

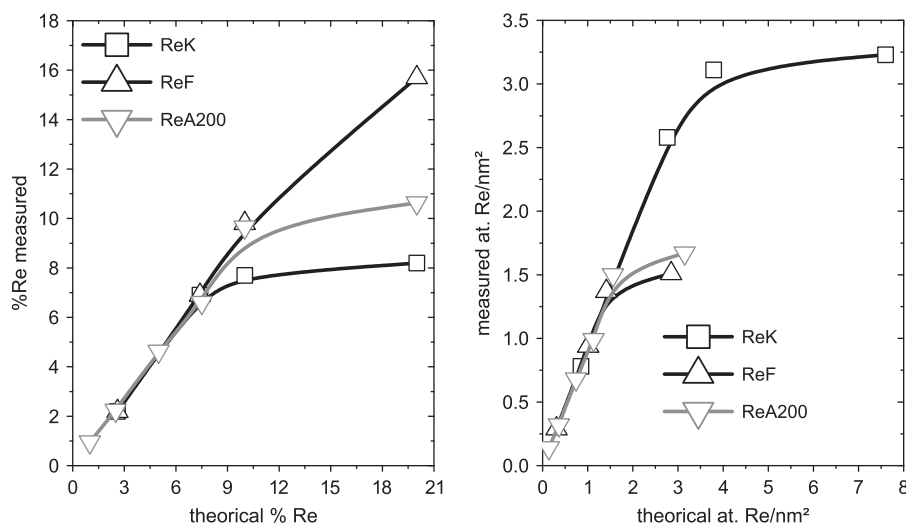


Fig. 1. Measured %Re content and Re surface coverage as a function of initial values for ReF, ReK and ReA200 catalysts.

### 3.2. In situ characterization of catalysts preparation

The catalysts preparation was monitored using TGA-DSC apparatus. For technical reasons, the calcination was performed by heating the  $\text{Re}^0+$  support mixture under a  $\text{N}_2/\text{O}_2$  flow (1:1) instead of pure  $\text{O}_2$ . Fig. 2 presents the mass loss derivatives for 6.9ReK and ReF materials. We have chosen this Re loading in order to compare our catalysts at iso-quantity of Re. First, a significant mass loss due to removal of physisorbed water from the support is observed up to 300 °C.

Between 300 and 380 °C, the samples weight increased with maximum rates at 334 °C (6.9ReF) and 344 °C (6.9ReK). These temperatures, reflecting the oxygen uptake maxima, are quite close to each other. Thus, the process occurs regardless the texture of the support and the bulk rhenium is efficiently oxidized around 340 °C. *In situ* Raman was used in order to shed light on the structural evolution of the catalyst during the preparation. The  $\text{Re}^0:\text{TiO}_2$  mixtures were heated up under pure  $\text{O}_2$  and the corresponding spectra are presented in Fig. 3. All spectra were normalized with regards to the total area of anatase features, observed at 146 (not shown), 395, 514 and 636  $\text{cm}^{-1}$  to take into account the broadening of the lines when increasing the temperature. Except from anatase contribution, no new Raman band of significant intensity is detected until the temperature reaches 350 °C. Because of the absence of Raman signal for  $\text{ReO}_2$  and  $\text{ReO}_3$  in this range [29], this is not an evidence of direct oxidation of  $\text{Re}^0$  to  $\text{Re}^{\text{VII}}$ .

When the temperature reaches 350 °C, a line assigned to terminal  $\text{Re}^{\text{VII}}=\text{O}$  stretch vibration,  $\nu_s(\text{Re}=\text{O}_t)$  is detected at 1008  $\text{cm}^{-1}$  (ReF) and 1005  $\text{cm}^{-1}$  (ReK). These frequencies fairly match the Raman signal of supported Re catalysts prepared using the Incipient Wetness Impregnation (IWI) method under dehydrated conditions [9].

After removal of the anatase contribution, it was possible to draw the evolution of the peaks detected at 1005 and 1008  $\text{cm}^{-1}$  as a function of temperature, as depicted in Fig. 4. Local maxima appeared below 300 °C, indicating the presence of superficial oxidized Re species, either supported onto metal Re or the support.

The presence of such local maxima suggests that the process involved is not alike a pure chemical vapor deposition (CVD), though occurs gradually and locally. Indeed, the oxidation and deposition of rhenium spreads from localized centers, making the parts of the sample analyzed under the microscope objective non-

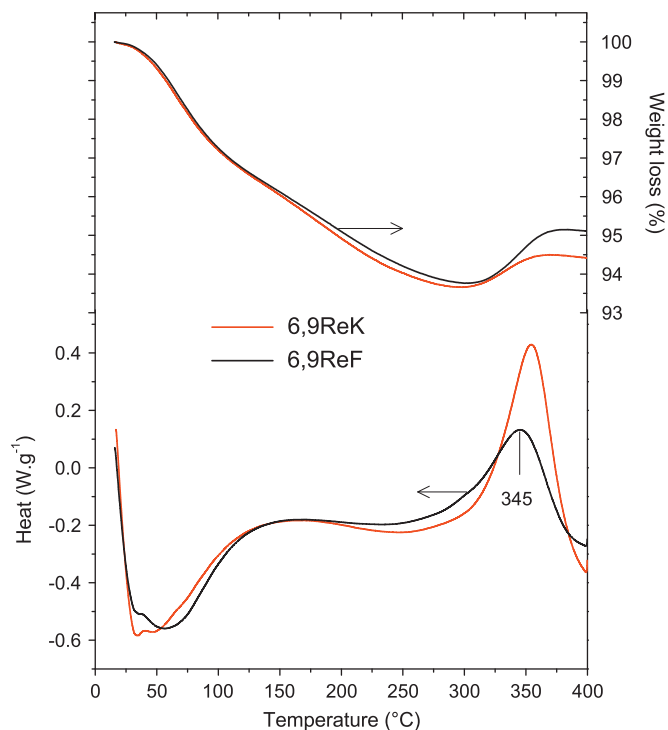


Fig. 2. Weight loss derivative and (top) and DSC profile (bottom) observed upon heating 6.9ReK (red line) and 6.9ReF (black line) catalysts. (For interpretation of the references to color in this figure legend, the reader is referred to the web version of this article.)

equivalent to each other. Both evolutions reach a maximum around 350 °C, which is in line with the oxygen uptake evidenced by the DSC profile. This relation shows that most of the rhenium is efficiently oxidized as  $\text{Re}^{7+}$  and simultaneously deposited onto the  $\text{TiO}_2$  surface.

### 3.3. Characterization of final catalysts

#### 3.3.1. TEM analysis

The TEM pictures of pure  $\text{TiO}_2$ -K03 support and the final 6.9ReK catalyst are presented in Fig. 5. Compared to the one of pure  $\text{TiO}_2$ , the picture of 6.9ReK material reveals very small dark

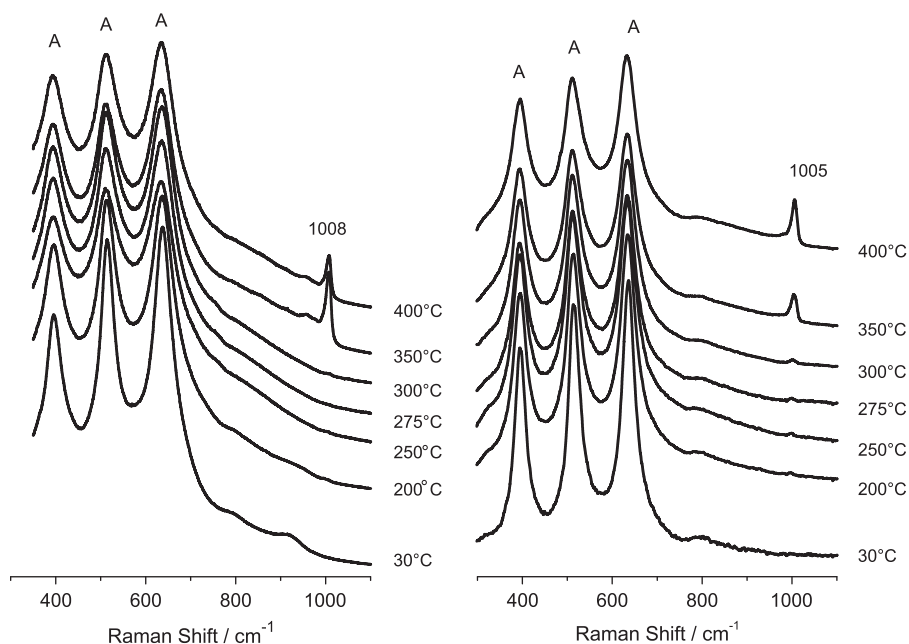


Fig. 3. Evolution of the Raman spectra of  $\text{Re}^0 + \text{TiO}_2\text{-F01}$  (left) and  $\text{Re}^0 + \text{TiO}_2\text{-K03}$  (right) mix upon heating under pure  $\text{O}_2$ .

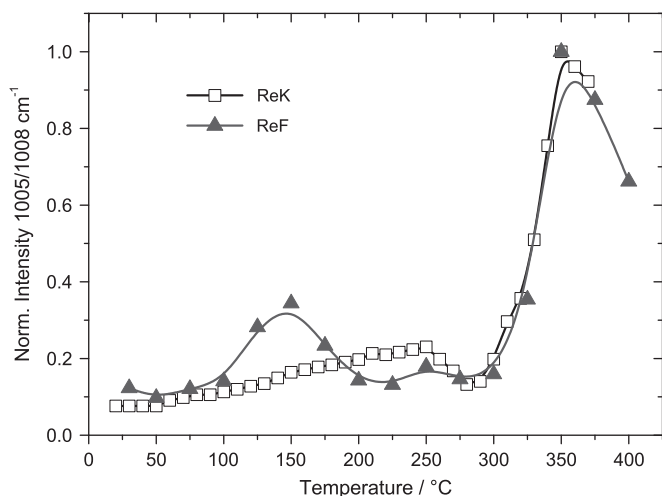


Fig. 4. Evolution of the Raman  $\nu_s(\text{Re}=\text{O}_t)$  line intensity as a function of temperature upon heating under pure  $\text{O}_2$ .

particles, whose diameter does not exceed 1 nm, which indicates the absence of sizeable  $\text{Re}^0$  domains.

### 3.3.2. UV-visible absorption

The optical absorption in the UV-visible range of fresh catalysts was measured under ambient conditions. Because of the huge absorption of the support  $\text{TiO}_2$  in the UV range, we have used the support  $\text{TiO}_2$  appropriately diluted in  $\text{BaSO}_4$  as 100% reflectance reference in order to make it possible to collect the absorption bands of the rhenium species in  $\text{Re}/\text{TiO}_2$  supported materials. However, the use of such a strong optical absorber as reference prevents any quantification attempt from the following data. The spectra of both 6.9ReF and 6.9ReK catalysts presented in Fig. 6 are dominated by an intense absorption in the UV region, which can be decomposed into several bands around 210, 240, 273 and 305 nm. In the case of high surface coverage 6.9ReK

material, an additional absorption is observed in the whole visible range with a maximum around 396 nm. Pure  $\text{ReO}_4^-$  in perfect Td coordination is known to have only two absorption bands below 300 nm, at 205 and 235 nm [26,27]. Upon distortion, degenerated transitions are generally observed between 200 and 300 nm with an enlargement to higher wavelengths (295 nm) [27]. The two materials thus mainly retain  $\text{ReO}_4^-$  moieties in distorted Td coordination under hydrated conditions. No absorbance in the visible range is detected, which confirms there is no rhenium remaining at the metallic state and supports the good dispersion of the rhenium oxide.

5ReA200 and 10.6ReA200 catalysts were examined accordingly as models for low and high coverage  $\text{Re}/\text{SiO}_2$  materials and the UV-vis absorption spectra are presented in Fig. 7. In this case, pure  $\text{SiO}_2\text{-Aerosil 200}$  was used as 100% reflectance reference.

The low loading material (5ReA200) exhibits a strong absorbance in the UV range due to two charge-transfer (CT) bands located at 210 and 238 nm, with no absorption in the visible. As detailed above, these bands feature non-distorted tetrahedral  $\text{ReO}_4^-$ . Increasing the loading produced a significant broadening of the UV bands towards the visible range and a shoulder is detected around 300 nm, revealing a certain degree of distortion. The 10.6ReA200 sample is also visibly colored and has an absorption in the visible range with maxima at 450 and 600 nm. According to [28], these energies could correspond to  $\text{Re}^{\text{IV}}$ .

### 3.3.3. Catalytic activity

The activities of 6.9ReF and 6.9ReK catalysts were tested in methanol conversion to dimethoxymethane (DMM). At low conversion levels, significant DMM selectivity were found in both materials as shown in Table 1. At higher conversion, differences are observed, which are related to the greater exposure of superficial  $\text{TiO}_x$  sites of the high surface area ReF catalyst, which leads to secondary reactions. The maximum conversion of ReA200 is rather low in so far as only 8% methanol conversion was detected at 260 °C. At low conversion, a balance between methylal (50%) and methylformate (50%) is observed, indicating that the selectivity of 6.6ReA200 towards DMM significantly lower than  $\text{Re}/\text{TiO}_2$  materials.

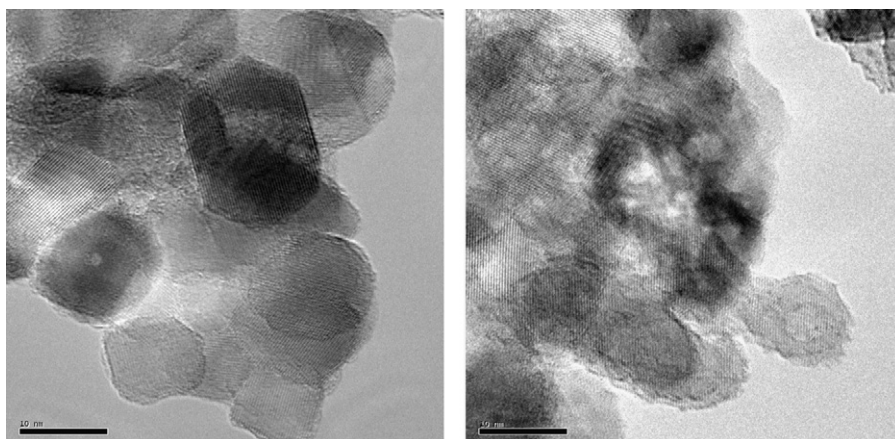


Fig. 5. TEM pictures of pure K03 anatase (left) and 6.9ReK catalyst after calcination (right).

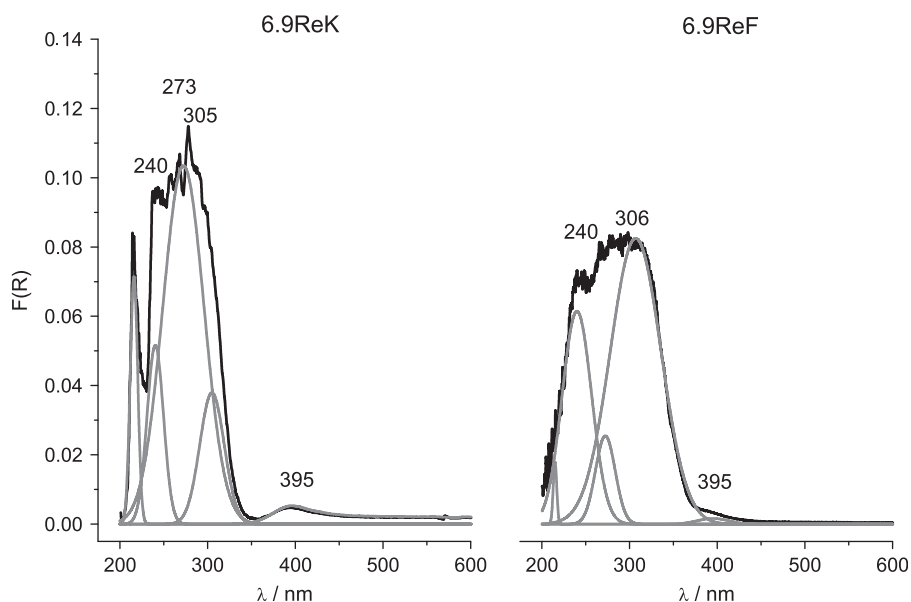


Fig. 6. Ambient UV-visible absorption spectra of fresh 6.9ReK (left) and 6.9ReF (right) catalysts and corresponding decomposition into Gauss curves.

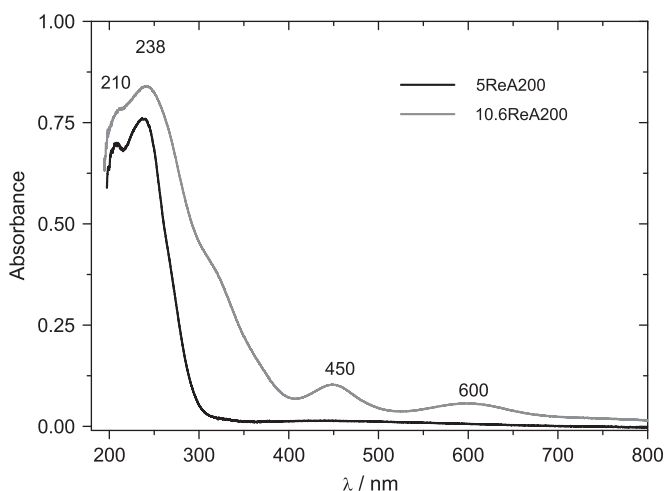


Fig. 7. Ambient UV-visible absorption spectra of (a) 5ReA200 and (b) 10.6ReA200 (right) catalysts under ambient conditions. Note: the spectra are not shifted.

The enhanced activity of  $\text{TiO}_2$  supported rhenium catalysts in comparison with  $\text{Re/SiO}_2$  materials for a given Re content is in line with the findings of Yuan and Iwasawa [6].

Table 1

Conversion and selectivity values for 6.6ReA200, 6.9ReF and 6.9ReK catalysts.

Catalyst	Temp. (°C)	Conv. (%)	$S_{\text{DME}}$ (%)	$S_{\text{F}}$ (%)	$S_{\text{MF}}$ (%)	$S_{\text{DMM}}$ (%)	$S_{\text{CH}_4}$ (%)	$S_{\text{CO}_x}$ (%)
6.9ReF	200	6.6	3.3	0.3	9.1	87.3	0	0
	260	32.3	8.3	5.2	21.7	54.8	0	10.0
6.9ReK	200	8.4	17.3	0	3.1	79.5	0	0
	260	44.3	12.1	1.2	7.8	76.7	0	2.0
6.6ReA200	200	<sup>a</sup>	–	–	–	–	–	–
	260	8	tr.	0	50	50	0	0

<sup>a</sup> The 6.6ReA200 only showed non-relevant, marginal activity.

#### 4. Discussion

The preparation technique we present here is the simplest one can imagine for preparing effective  $\text{Re/TiO}_2$  and  $\text{Re/SiO}_2$  catalysts. The Re loss during the preparation is significant, especially for high rhenium initial contents, and is more pronounced for high BET surface supports. At low surface coverage and under dehydrated conditions, there is no evidence of different anchoring of the oxorhenate phase onto the support,  $\text{SiO}_2$  or  $\text{TiO}_2$ .

DSC and confocal Raman spectroscopy suggest the synthesis of the catalyst involved both  $\text{Re}^0$  particle gradual superficial oxidation and a CVD-like process in which the metallic rhenium volatilizes as  $\text{Re}_2\text{O}_7$  before deposition. Indeed, the deposition of Re occurs in two stages. Below 300 °C, a minority of localized superficial  $\text{Re}^{\text{VI}}\text{O}_4$  species are already present as reflected by a moderate increase of  $\nu(\text{Re}=\text{O}_t)$  modes in the confocal Raman spectra. This stage could correspond to a gradual oxidation of  $\text{Re}^0$  particles, probably from the surface along an onion-like depiction, and subsequent deposition of  $\text{ReO}_4$  moieties onto the support. A marked maximum oxygen uptake is evidenced by both techniques between 300 and 350 °C, which could be assigned to the complete oxidation of  $\text{Re}^0$  to gaseous  $\text{Re}_2\text{O}_7$  simultaneously to rhenium oxide deposition.

Upon hydration, the structure of the as prepared catalysts is found to be affected by both the rhenium surface coverage and the nature of the support as evidenced by UV–vis absorption spectroscopy. At low surface coverage, only  $\text{O} \leftarrow \text{Re}$  charge-transfer (CT) bands are observed in the UV assigned to isolated  $\text{ReO}_4^-$  species. In the case of  $\text{TiO}_2$ -supported 6.9ReF catalyst, the structure is distorted from a pure Td coordination, which would be the case for a dehydrated oxorhenate phase. On the opposite, the rhenium oxide in 5ReA200 is alike fully hydrated, free  $\text{ReO}_4^-$  anions, suggesting the  $\text{ReO}_x$  phase is significantly more subjected to hydration when supported onto  $\text{SiO}_2$ . This could explain the differences observed in the catalytic performances between  $\text{TiO}_2$  and  $\text{SiO}_2$  supported catalysts. The extreme volatility of hydrated rhenium oxide could be responsible of a dramatic rhenium loss in the case of  $\text{Re}/\text{SiO}_2(\text{Aerosil-200})$  catalyst and hence, disable the catalytic activity of the material. Indeed, after the catalytic test, the rhenium content as measured by ICP was as low as 734 ppm in the case of 5ReA200 and 0.2%wt in the case of 20ReA200 material. This trend fairly supports the findings of Lee and Wachs [24], who observed such a dramatic loss of rhenium in  $\text{Re}/\text{SiO}_2$  when subjected to moisture. As a consequence, the authors could not achieve a complete isotopic oxygen exchange of the superficial oxorhenate species with  $\text{H}_2^{18}\text{O}$ .

## 5. Conclusion

This study presents a simple and reliable way to prepare supported oxorhenate catalysts on the base of a dry process. Because of the extreme volatility of  $\text{HReO}_4$ , this route appears to be a good alternative in comparison with the use of an aqueous rhenium oxide precursor. The structures and the catalytic activity in methanol conversion of the resulting materials are comparable to those of catalysts prepared using the IWI technique. Our results strongly suggest the rhenium deposition occurs via an oxidative thermal spreading coupled with a CVD-like process regardless the support. The use of such a “dry” process has allowed highlighting the similarities between  $\text{TiO}_2$  and  $\text{SiO}_2$  support as long as the

catalyst is maintained in dehydrated conditions. Conversely,  $\text{TiO}_2$  and  $\text{SiO}_2$  have shown clear disparities towards hydration, either induced by the reaction or exposure to ambient conditions. At low surface coverage, the rhenium oxide phase consists in isolated species in Td coordination, while clusters embedding several oxidation states cannot be excluded at higher Re loadings. The presence of clusters was shown to favor the direct conversion of methanol to methylal.

## Acknowledgments

This work was supported by the French Ministry for Education and Research as Ph.D. grants allocated to Dr. Sécordel and Mr. Yoboué. O. Gardoll and M. Trentesaux are gratefully acknowledged for their technical expertise for the DSC and XPS analyses, respectively. The present work was also supported by the IDECAT European network.

## References

- [1] N.S. Wang, C.S. Laufer, *Industrial Bioprocessing* 27 (4) (2005) 6–7.
- [2] A.P. Soares, M.F. Portela, A. Kiennemann, *Catal. Rev.* 47 (2004) 125–174.
- [3] Haichao Liu, Enrique Iglesia, *J. Phys. Chem. B* 109 (6) (2005) 2155–2163.
- [4] Y. Fu, J. Shen, *Chem. Commun.* (2007) 2172–2174.
- [5] Y. Yuan, T. Shido, Y. Iwasawa, *Chem. Commun.* (2000) 1421–1422.
- [6] Y. Yuan, Y. Iwasawa, *J. Phys. Chem. B* 106 (2002) 4441–4449.
- [7] S. Royer, X. Sécordel, M. Brandhorst, F. Dumeignil, S. Cristol, C. Dujardin, M. Capron, E. Payen, J.-L. Dubois, *Chem. Commun.* (2008) 865–867.
- [8] B. Mitra, X. Gao, I.E. Wachs, A.M. Hirt, G. Deo, *Phys. Chem. Chem. Phys.* 3 (2001) 1144–1152.
- [9] X. Sécordel, E. Berrier, M. Capron, S. Cristol, J.-F. Paul, M. Fournier, E. Payen, *Catal. Today*, 155 (2010) 177–183.
- [10] I.E. Wachs, *Catal. Today* 27 (1996) 437–455.
- [11] N. Viswanadham, T. Shido, Y. Iwasawa, *Appl. Catal. A: General* 219 (2001) 223–233.
- [12] T. Kusakari, T. Sasaki, Y. Iwasawa, *Chem. Commun.* (2004) 992–993.
- [13] H.S. Lacheen, P.J. Cordeiro, E. Iglesia, *J. Am. Chem. Soc.* 128 (4) (2006) 15082–15083.
- [14] H.S. Lacheen, P.J. Cordeiro, E. Iglesia, *Chem. Eur. J.* 13 (2007) 3048–3057.
- [15] H. Balcar, R. Hamtil, N. Žilková, J. Čejka, *Catal. Lett.* 97 (2004) 25–29.
- [16] R. Hamtil, N. Žilková, H. Balcar, J. Čejka, *Appl. Catal. A: General* 302 (2) (2006) 193–200.
- [17] C.-B. Wang, Y. Cai, I.E. Wachs, *Langmuir* 15 (1999) 1223–1235.
- [18] J. Okal, L. Kepiński, L. Krajczyk, M. Drozd, *J. Catal.* 188 (1999) 140–153.
- [19] J. Okal, J. Baran, *J. Catal.* 203 (2001) 466–476.
- [20] J. Okal, *Appl. Catal. A: General* 287 (2005) 214–220.
- [21] M.A. Vuurman, D.J. Stufkens, A. Oskam, I.E. Wachs, *J. Mol. Catal.* 76 (1–3) (1992) 263–285.
- [22] B. Mitra, X. Gao, I.E. Wachs, A.M. Hirt, G. Deo, *Phys. Chem. Chem. Phys.* 3 (2001) 1144–1152.
- [23] E.L. Lee, I.E. Wachs, *J. Phys. Chem. C* 111 (2007) 14410–14425.
- [24] E.L. Lee, I.E. Wachs, *J. Phys. Chem. C* 112 (2008) 6487–6498.
- [25] M. Valigi, D. Cordischi, D. Gazzoli, C.P. Keijzers, A.K. Klaassen, *J. Chem. Soc.* 1981 (77, 1871).
- [26] M. Stoyanova, U. Rodemerck, U. Bentrup, U. Dingerdissen, D. Linke R.-W. Mayer, H.G.J. Lansink Rotgerink, T. Tacke, *Appl. Catal. A: General* 340 (2008) 242–249.
- [27] N. Escalona, J. Ojeda, R. Cid, G. Alves, A. López Agudo, J.L.G. Gil Llambias, *Appl. Catal. A: General* 234 (2002) 45–54.
- [28] R.M. Edreva-Kardjeva, A.A. Andreev, *J. Mol. Catal.* 46 (1988) 201–207.
- [29] M. Ishii, T. Tanaka, T. Akahane, N. Tsuda, *J. Phys. Soc. Jpn.* 41 (1976) 908–912.